JOURNAL OF MATERIALS SCIENCE 17 (1982) 2817–2824

Microstructural study of a high-strength stress-corrosion resistant 7075 aluminium alloy

K. RAJAN, W. WALLACE, J. C. BEDDOES
National Aeronautical Establishment, National Research Council, Canada, Ottawa, Ontario, KIA OR6, Canada

A heat-treatment procedure providing for enhanced stress-corrosion cracking resistance without any sacrifice of yield strength in 7075 aluminium alloy is investigated using transmission electron microscopy. It is suggested that the heat treatment (known as retrogression and re-ageing) provides for large grain-boundary precipitates and coherent matrix precipitates. The latter provides for the high strength levels while the grain-boundary precipitates provide for enhanced stress-corrosion cracking resistance. A hydrogen embrittlement mechanism of stress-corrosion cracking is assigned to this alloy system.

1. Introduction

Alluminium alloys of the 7075 type (Al–Zn–Mg–Cu) are widely used in airframe structures. They provide very high strength and stiffness, but are prone to stress-corrosion cracking (SCC), particularly when aged to the near peak strength T6 condition. Their resistance to stress-corrosion cracking can be increased by over-ageing to the T73 temper, but with a progressive loss of strength. For example, the yield strength of 7075-T73 is about 10–15% lower than that of 7075-T6.

Cina [1] has reported a heat treatment known as retrogression and re-ageing (RRA), which was claimed to give stress-corrosion resistance in 7075 aluminium equivalent to the T73 temper, together with T6 strength levels. This treatment is applied to material in the T6 condition and consists of a short-time heat treatment at a temperature in the range 200–280° C, followed by re-ageing using the same conditions used for the original T6 age. The heat-treatment conditions used for the standard T6 and T73 tempers are given in Table I. Fig. 1 shows schematically the variations in hardness or yield strength observed during retrogression and re-ageing. During retrogression, strength falls very rapidly to reach a minimum before increasing again to a secondary peak, and then decreasing again at long times as the material over-ages. On re-ageing after short retrogression treatments, strength can be restored to original T6 levels, while longer retrogression times lead to a gradual loss of re-ageing responses, as indicated in Fig. 1. It was claimed by Cina that processing to the minimum of the retrogression curve, followed by re-ageing led to the favourable combination of T6 strength and T73 stress-corrosion resistance.

The time required to reach the minimum on the retrogression curve varied with temperature, but was of the order of 5 to 6 sec. This would effectively restrict the process to thin sheet, while 7075 aluminium is used primarily for thick section components. Previous work done in this laboratory [2], applied the RRA treatments using lower retrogression temperatures. This would allow longer times to be used for thicker material. It was found at lower temperatures (down to 160° C) that similar RRA trends can be observed and thus these treatments are applicable to thicker sections. The results of the previous study may be summarized as follows.

TABLE I Heat-treatment options for 7075

T6:	Solution treat, quench and age (120° C/29 h) to 'peak' strength
T73:	Solution treat, quench and two-stage over-age (110° C/8 h + 177° C/8 h) to improve stress-corrosion resistance

0022–2461/82/102817–08$03.46/0

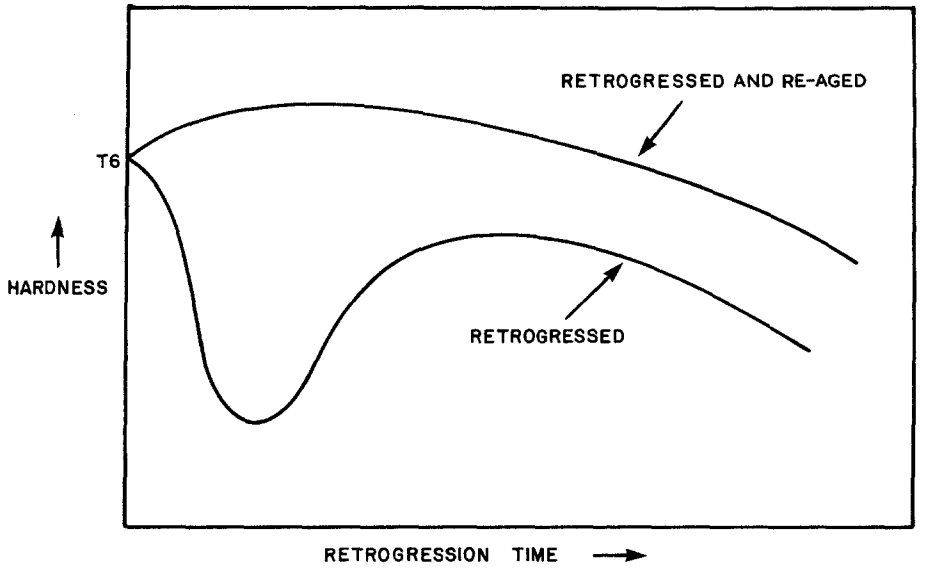

Figure 1 Schematic representation of the change in hardness during retrogression and re-ageing.

The traditional trade-off between SCC resistance and yield strength, in choosing between T73 and T6 tempers, is not always necessary. By using RRA treatments stress-corrosion crack-growth rates very similar to the T73 condition can be obtained without sacrificing T6 strength. However, in the heats studied, the initial minimum in the retrogressed strength curve did not correspond to the retrogression time giving the optimum combination of strength and stress-corrosion resistance. By using low retrogression temperatures (160 and 180° C) the kinetics of the reaction occurring during retrogression are retarded, allowing longer times. However, at the lower temperatures T73, stress-corrosion resistance was only obtained by sacrificing yield strength about 6%.

The aim of the present study was to examine the cause for the improvement in SCC resistance using the RRA treatments. Besides the T6 and T73 conditions, samples in the RRA and just retrogressed conditions showing the best SCC resistance were examined by transmission electron microscopy. By such an examination, the microstructural parameters governing stress-corrosion cracking may be defined.

2. Experimental details

Heat treatments were carried out on un-machined specimens from 1.9 cm diameter T6 bar or 2.5 cm thick T651 plate. Silicone oil baths were used. Specimens for mechanical testing were machined after full heat treatment. The details of the heat treatments and mechanical testing are described elsewhere [2]. Specimens for transmission electron microscopy were made by conventional methods of jet electropolishing, using a solution of 33% nitric acid in methanol at −25° C. The alloy composition is given in Table II.

3. Experimental results

3.1. Mechanical testing

In previous work the effects of different retrogression temperatures were studied. From these experiments it was concluded that the microstructural changes taking place during retrogression occur faster and to a greater extent at higher retrogression temperatures. In this report, the microstructural effects at the highest retrogression temperature (220° C) studied, are reported, as this produced the best SCC resistance.

The effects of retrogression and RRA on yield strength are summarized in Fig. 2. It is clear from this that the general shape of the retrogression

TABLE II Composition limits of aluminium alloy 7075

Element	wt %
Zn	5.1–6.1
Mg	2.1–2.9
Cu	1.2–2.0
Fe	0.5
Si	0.4
Mn	0.3
Cr	0.18–0.28
Ti	0.2
Al	Balance

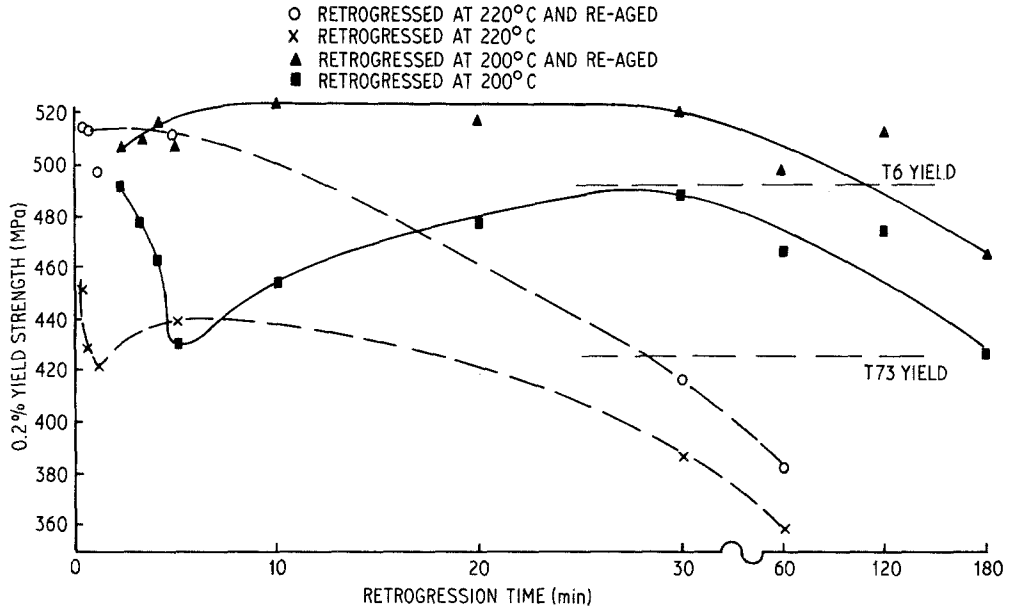

Figure 2 Measured changes in yield strength during retrogression and re-ageing.

curves is similar to the hardness curves obtained by Cina. The RRA material has yield strengths which are higher than the minimum T6 values and the as-received T6 value for the sample tested. The results are shown here for the 200 and 220° C heat treatments.

The stress-corrosion test data reported here are for T651 material heat treated at 220° C as this was the temperature initially suggested by Cina for producing good SCC results. The SCC crack-growth data are shown in Fig. 3. Among the materials retrogressed at 220° C, the 5-min heat

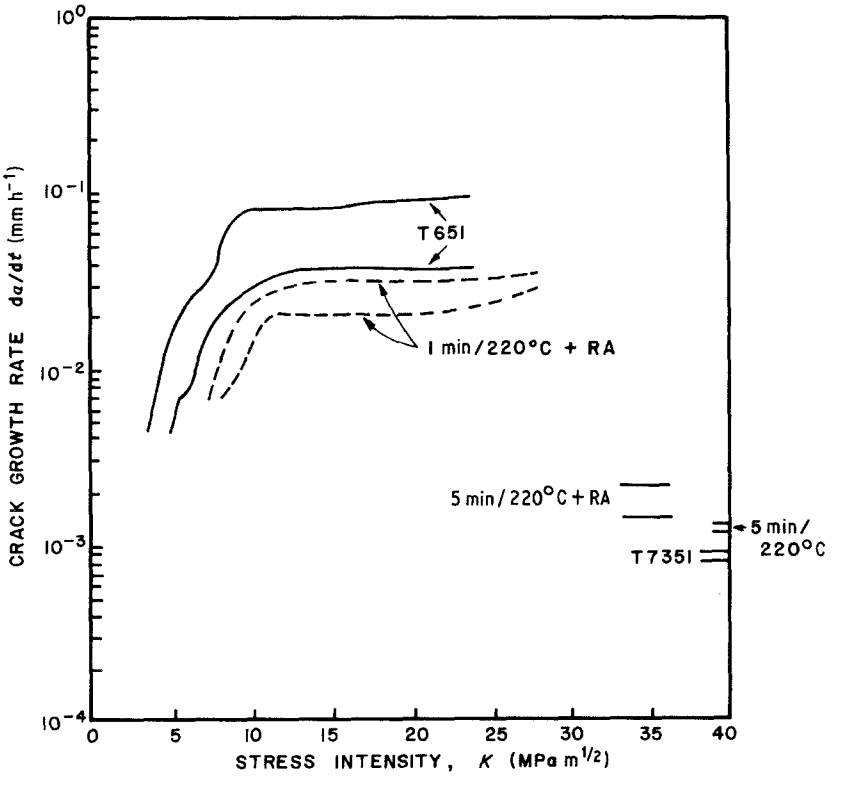

Figure 3 Stress-corrosion crack-growth rates for the heat treatments examined in this study.

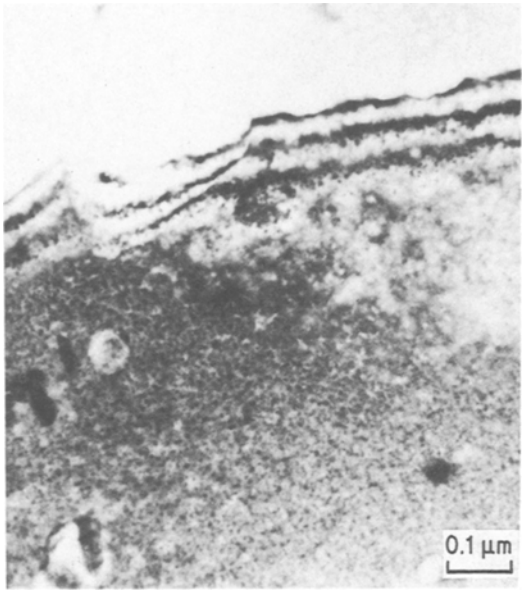

Figure 4 Bright-field micrograph showing coherent precipitates in retrogressed and re-aged material $g = (1\,1\,1)$.

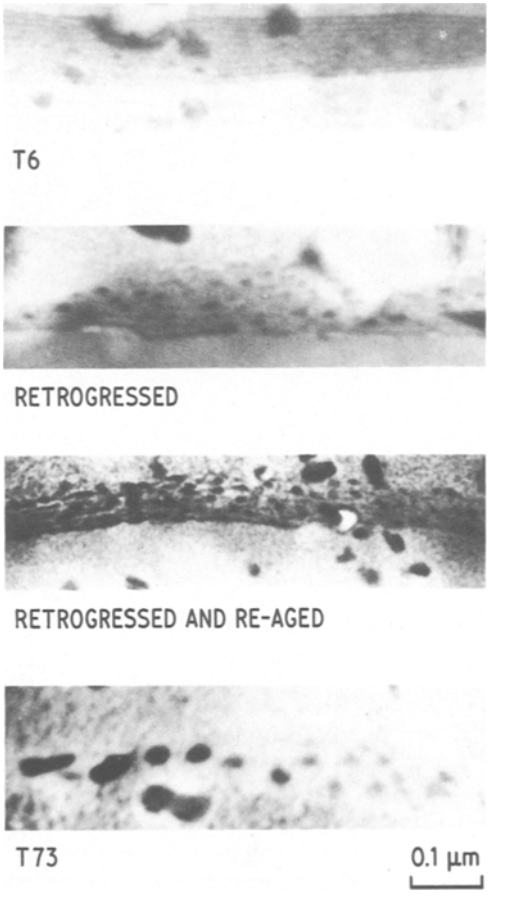

Figure 5 Typical grain-boundary precipitate structures in the heat-treatment conditions examined in this study.

treatment produced the best SCC results. As can be seen in Fig. 2 this does not correspond to the minimum in the retrogression curve at 220° C. This would indicate that the retrogression minimum in itself is not a significant point in terms of stress-corrosion cracking resistance.

The RRA material produced SCC results comparable to the retrogressed material yet without the loss in strength compared to the T6 (or T651). Thus the RRA treatment of T6 (or T651) provides SCC results similar to T73 without loss in mechanical strength.

3.2. Transmission electron microscopy

As mentioned earlier, the electron microscopy was conducted on the material subjected to tensile tests, i.e. T6, T73, retrogressed 5 min at 220° C, and RRA given the same retrogression treatment.

Microscopy has shown that the significant effects of the heat treatments were upon grain-boundary precipitate size and upon the presence of coherent precipitates in the matrix. The T6 and T73 conditions exhibited the conventional microstructures with the coherent precipitate structure in the T6 and the over-aged structure in the T73 with η and η'. The retrogressed and re-aged material has a matrix structure of coherent precipitates (Fig. 4). This would account for strength levels equivalent to that of T6 and higher.

While the mechanical strength improvements upon RRA can be correlated to the matrix structure, the SCC results need to be examined in the context of grain-boundary structure. The only significant difference between the different conditions examined was in grain-boundary precipitate size (Fig. 5). The average grain-boundary particle sizes for each treatment are listed in Table III. The T6 condition has the smallest precipitate size while T73 has the largest. However, what should be brought to attention is that those heat treatments producing the better SCC results have a significantly larger grain-boundary precipi-

TABLE III Effect of heat treatment on grain-boundary precipitate size

Heat treatment	Grain-boundary precipitate size (nm)
T6	1400
Retrogressed: 5 min, 220° C	2300
Retrogressed and re-aged	2400
T73	3000

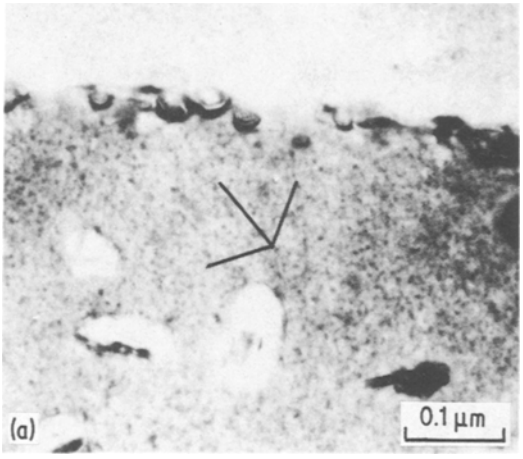

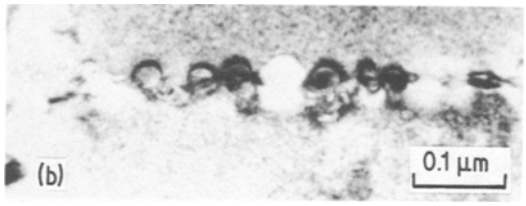

Figure 6 Hydrogen-bubble development after exposure of thin foil to laboratory air after many weeks. (a) Bubble morphology shape following traces of {1 1 1} planes. $g = (1\,3\,1)$ for lower grain. (b) Strain-field image exhibiting Ashby–Brown contrast. Note that the line of no constrast is in the boundary plane. $z = [1\,1\,0]$ $g = (1\bar{1}\,3)$ for lower grain.

tate size than the T6 condition which has poor SCC results.

These results are similar to those described by Christodoulou and Flower [3] in their study of Al–Zn–Mg alloys exposed to moist atmospheres. These workers correlated grain-boundary precipitate size to hydrogen-bubble nucleation leading to enhanced tensile ductility. In fact they found that a critical grain-boundary particle size of approximately 20 nm is needed for bubble nucleation. It is interesting to compare this with what is found in the present study, since the heat treatments producing the better SCC results had an average grain-boundary precipitate size greater than 20 nm. However, Christodoulou and Flower found a concurrent loss in strength with the increase in ductility in both dry and wet conditions with over-ageing. The heat treatments in the present study, however, have not produced improvements in SCC resistance at the expense of strength as is usually the case.

4. Discussion

The examination of the microstructure suggests that the retrogression treatment is a precipitate-coarsening treatment for grain-boundary precipitates. The re-ageing of the retrogressed material allows for the nucleation and growth of coherent precipitates in the matrix. The latter effects strengthening by conventional mechanisms while it may be postulated that stress-corrosion cracking is controlled by the grain-boundary precipitate size. It is the microstructural effects on stress-corrosion cracking that this discussion will focus on. The results of the present study may be interpreted in terms of hydrogen-embrittlement concepts.

Central to the concept of hydrogen embrittlement and its application to stress-corrosion cracking, is the relative effect of hydrogen in solution in atomic form compared to it being in molecular form as a gas. It has been suggested that the latter is better in terms of SCC resistance as hydrogen in solution enhances decohesion of the metallic bonds. Given this premise, the microstructural characterization of trapping sites is essential to understanding the role of hydrogen embrittlement.

The concepts of hydrogen trapping have been discussed extensively in the literature [4, 5]. In trying to characterize hydrogen-trapping sites in relation to stress-corrosion crack-growth data, it is useful to utilize the concept of reversible and irreversible traps. The reversible trap is one at which hydrogen has a short residence time while with an irreversible one, the release of the hydrogen atom once it is captured is highly improbable [6]. The higher the density of irreversible sites, the higher the probability of hydrogen capture.

In this work it may be said that an increase in particle size increases the fraction of irreversible sites. Thus more hydrogen is trapped or captured as the particle size increases. Since the fraction of irreverisible sites is associated with particle size, it is the particle/matrix interface that provides the trapping sites. As the grain-boundary precipitates grow larger, the degree of incoherency around the particles increases. It is proposed that the accumulation of dislocations at the particle/matrix interface provides the trapping sites for hydrogen. Although the microstructural study presented here was not aimed at examining material exposed to the environment, it was noteworthy that some of the thin foils exposed to laboratory air for many weeks did exhibit what appeared to be bubbles at grain boundaries (Fig. 6). The other workers, upon

examining material exposed to a wet environment, have observed identical images as seen here and have described them as bubbles of molecular hydrogen [3, 7–9]. The bubbles were visible by Ashby–Brown [10] strain-field contrast in bright-field with the line of no contrast lying in the grain-boundary plane rather than normal to the operating reflection. Also, as found by Scamans [9], the bubble morphology was most evident when using high-index reflections in bright-field. Also, it was apparent that the bubble was hexagonal in shape bounded by [1 1 1] planes, also noted by Scamans. A more systematic study is presently under way to examine bubble formation. However, suffice it to say that the results presented here provide some support to the concept of hydrogen trapping in this alloy system.

The description of hydrogen trapping as being associated with defect structure is consistent with those proposed by other workers. Kumnick and Johnson [11], in studying hydrogen trapping in iron, suggested that trapping sites are probably associated with inelastic interaction of hydrogen with dislocation cores or with point defects. By using time-lag measurements based upon gas-phase charging and electrochemical measuring techniques, these workers postulated that the traps were associated with the imperfection structure that developed during plastic deformation. Wampler *et al.* [12], in examining hydrogen trapping in copper, confirmed the suggestion of Greenwood *et al.* [13], that dissolved gas atoms will be attracted by the tensile strain field of a dislocation. Work by Robertson [14] on TD nickel showed that the particle/matrix interface can be a hydrogen-trapping site. In that case the structure of the interface is affected by plastic deformation. The greater the degree of plastic deformation the more the hydrogen was withdrawn from solution. It was suggested that cold work produces voids which would allow more hydrogen to be trapped.

The possible effects of the degree of coherency at the precipitate/matrix interface on hydrogen trapping have been suggested by other workers. For example, Rath and Bernstein [15] have pointed out that coherent TiC particles in steel are not as effective as hydrogen traps as incoherent ones. The large TiC particles are considered as irreversible hydrogen traps characterized by a large interaction energy (TiC–H) and consequently a long hydrogen residence time unlike the smaller TiC particles. The same may hold true for the larger grain-boundary precipitates in the 7075 aluminium alloy.

The crack-growth data of the present study, produced by the different heat treatments, may be interpreted on the basis of the availability of hydrogen-trapping sites. Hydrogen dissolves in the metal at the crack tip where the metal is exposed to the environment. The dislocations generated at the crack tip pick up the hydrogen. Assuming that crack-growth propagation is boundary sensitive, the presence of trapping sites at grain boundaries is important. The crack tip dislocations carry the hydrogen atoms into the metal ahead of the crack tip. If the hydrogen is trapped on an irreversible site then the dwell time of hydrogen on the trapping site is long. If the site is a reversible one, then the dwell time is short. When the crack reaches the trapping site it will "see" hydrogen in the metal if the site is a reversible one. At an irreversible site, there is little hydrogen in solution and the cohesive strength of the metal is higher, thus inhibiting crack growth. Keeping in mind that the crack tip is constantly exposed to the environment, the rate of embrittlement will be controlled by the rate of hydrogen entry into the metal. Thus time must be allowed for the hydrogen in the metal to be carried to the trapping site by the crack-tip dislocations. This would mean that the rate of embrittlement is controlled by the rate of entry of hydrogen through the surface film on the walls of the crack. This suggestion is in agreement with the work of Gest and Troiano [16] and Scamans *et al.* [7].

When the crack approaches a large grain-boundary precipitate (that is, an irreversible hydrogen trap), the crack growth is retarded. Temporary crack arrest may occur each time a hydrogen bubble is reached because of crack-tip blunting. Consequently, this would lead to discontinuous crack growth by the hydrogen-embrittlement mechanism as proposed in this study. The model presented here may be interpreted in terms of atomic decohesion at crack tips in the presence of atomic hydrogen. In fact this has been suggested by Fuller *et al.* [17] for explaining the enhanced crack growth in steels when hydrogen is introduced into the environment in atomic rather than molecular form.

While the preceding discussion has focused on the hydrogen-embrittlement mechanism, it would be worthwhile to consider the possibility of a dissolution controlled SCC mechanism as well. As

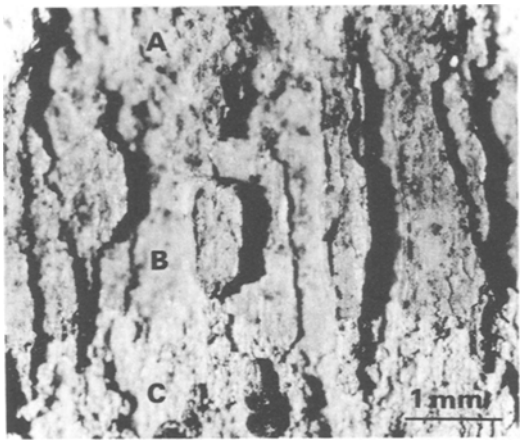

Figure 7 Fractograph showing intergranular separation in RRA material. The intergranular mode is promoted by stress-corrosion while the transgranular regions of the fracture surface are stress generated. A, starter crack region; B, SCC region; C, overload region.

has been pointed out by Scully [18] a dissolution-controlled mechanism arises from the interaction between a plastically strained metal and the solution. In such circumstances, crack propogation tends to be transgranular.

The hydrogen-embrittlement mechanism proposed in this study suggests a grain-boundary sensitive fracture mode. Fig. 7 shows an SCC fracture surface of RRA material. It must be kept in mind that we are looking at crack propogation in the short transverse rolling direction. Thus what we see on the fracture surface are not only the transgranular regions but also the grain faces of the elongated grains, indicating intergranular separation. A schematic diagram of the fracture path is indicated in Fig. 8. Stress corrosion promotes an intergranular fracture mode but the transition to a transgranular mode is stress generated.

The consideration of the crack path is in itself not sufficient to distinguish between the hydrogen embrittlement and dissolution-controlled SCC mechanisms. However, the evidence of hydrogen trapping, the presence of intergranular separation on the SCC fracture surface and supporting evidence in previously published work as discussed in this paper, collectively suggest that a hydrogen-embrittlement mechanism of stress-corrosion cracking may be assigned to this alloy system.

5. Conclusions

(1) The results of the retrogression and re-ageing treatments of 7075 aluminium alloy suggest that the traditional trade-off between stress-corrosion cracking resistance and yield strength in choosing between T73 and T6 tempers is unnecessary.

(2) The improvement in stress-corrosion cracking resistance correlates well with the increase in grain-boundary precipitate size.

(3) The defect structure associated with the incoherency of the precipitate/matrix interface can act as trapping sites for hydrogen, where bubbles of gaseous hydrogen can form.

(4) Enhancing grain-boundary precipitation is necessary in producing a microstructure resistant to hydrogen embrittlement. Since grain-boundary defects can affect second-phase nucleation, enhancing the mobility of such defects should promote grain-boundary precipitation. This is an area of further investigation.

References

1. B .M. CINA, US Patent 3856584, 24 December (1974).
2. W. WALLACE, J. C. BEDDOES and M. C. DEMALHERBE, *Canad. Aeronout. Space Inst.* **27** (1981) 222.
3. L. CHRISTODOULOU and H. M. FLOWER, *Acta Metall.* **28** (1980) 481.
4. G. M. PRESSOUYRE and I, M. BERNSTEIN, *ibid.* **27** (1979) 89.

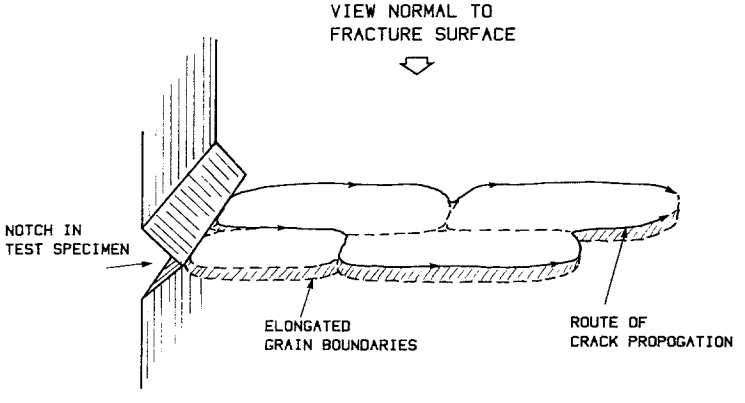

Figure 8 A schematic diagram indicating the path of crack propagation in the SCC test samples.

5. G. M. PRESSOUYRE, *ibid.* **28** (1980) 895.
6. G. M. PRESSOUYRE and I. M. BERNSTEIN, *Met. Trans.* **9A** (1978) 1571.
7. G. M. SCAMANS, R. ALANI and P. R. SWANN, *Corros. Sci.* **16** (1976) 443.
8. R. ALANI and P. R. SWANN, *Br. Corros. J.* **12** (2) (1977) 80.
9. G. M. SCAMANS, *J. Mater. Sci.* **13** (1978) 27.
10. M. F. ASHBY and L. M. BROWN, *Phil. Mag.* 8 (1963) 1083.
11. A. J. KUMNICK and H. H. JOHNSON, *Acta Metal.* **28** (1980) 33.
12. W. R. WAMPLER, T. SCHOBER and B. LENGELER, *Phil. Mag.* **34** (1976) 129.
13. G. W. GREENWOOD, A. J. E. FOREMAN and D. E. RIMMER, *J. Nucl. Mater.* 4 (1959) 305.
14. W. M. ROBERTSON, *Met. Trans.* **10A** (1979) 489.
15. B. B. RATH and I. M. BERNSTEIN, *ibid.* **2** (1972) 2845.
16. R. GEST and A. R. TROIANO, Proceedings of the International Congress on Hydrogen in Metals, 29 May–2 June 1972 (Editions Science et Industrie, Paris, 1972) p. 427.
17. E. R. FULLER, Jr, B. R. LAWN and R. M. THOMSON, *Acta Metal.* **28** (1980) 1407.
18. J. C. SCULLY, in "Mechanisms of Environment Sensitive Cracking of Materials", edited by P. R. Swann, F. P. Ford and A. R. C. Westwood (Metals Society, London, 1977) p. 1.

Received 27 November 1981
and accepted 8 February 1982